APPENDIX FOR:

"NSMCE2 suppresses cancer and aging in mice independently of its SUMO ligase activity"

Ariana Jacome, Paula Gutierrez-Martinez, Federica Schiavoni, Enrico Tenaglia, Paula Martinez, Sara Rodriguez, Emilio Lecona, Matilde Murga, Juan Mendez, Maria A. Blasco & Oscar Fernandez-Capetillo

TABLE OF CONTENTS

Appendix Figure S1. Expression of NSMCE2 in murine and human tissues

(**a**) Western blot using the monoclonal anti-human NSMCE2 developed in this study in U2OS cells after transfection with 3 independent siRNA sequences. β-actin was used as a loading control. (**b**) IHC in human tissues using the NSMCE2 antibody shown in (**a**). The expression of NSMCE2 is highest in proliferating areas such as lymph nodes or the proliferating areas of skin and ovary. In addition, NSMCE2 is distinctively high in spermatocytes. Scale bar indicates 100 μm. (**c**) Expression of NSMCE2 in mouse 13.5 dpc embryos using an independent polyclonal antibody against the murine protein. The expression of NSMCE2 is again highest in areas of intense proliferation (revealed by Ki67 staining), such as the developing brain. The specificity of this antibody was validated by its lack of reactivity in NSMCE2 deficient cells (see main Figs. 2, 5). Scale bar indicates 100 μm.

Appendix Figure S2. Induction of NSMCE2 foci by catalytic inhibition of topoisomerase activity

The images illustrate the staining pattern of NSMCE2 and BRCA1 in wt MEF exposed to ICRF-193 (5 μM, 2 hrs), a catalytic inhibitor of TOP2A. Scale bar indicates 2.5 μm.

Appendix Figure S3. SUMO ligase activity of the NSMCE2 C185S/H187A mutant

(**a**) Outline of the process used to evaluate the SUMO ligase activity of wild type and C185S/H187A (NSMCE^{SD}) mutant proteins. Wt and mutant cDNAs expressing both proteins were cloned directly from RNA obtained from wt and *Nsmce2*$^{SD/SD}$ MEF, and subsequently expressed in HEK293T cells. Clones expressing similar amounts of wt and mutant NSMCE2 were selected. EGFP-SUMO1 or Flag-SUMO2 were transfected into these clones, and were used to pull down SUMOylated proteins using immunoprecipitation. The SUMO ligase activity was evaluated by looking at NSMC2 autosumoylation. (**b**) The panels illustrate the SUMO ligase activity of the wt and SUMO protein when evaluated as explained in (**a**). Whereas NSMCE2 SUMOylation with SUMO2 is fully

absent on the NSMCE^{SD} mutant, some residual activity can be detected when using overexpressed SUMO1. However, these experiments are done on the context of endogenous NSMCE2 from HEK293T cells and this activity could derive from the endogenous protein. Nevertheless, we note that this is the very same mutation that has been used as a SUMO deficient strain (Andrews et al, 2005; Branzei et al, 2006; Kegel et al, 2011; Pebernard et al, 2008; Takahashi et al, 2008).

Appendix Figure S4. NSMCE2 foci formation in wt and *Nsmce2*$^{SD/SD}$ MEF

High-Throughput Microscopy (HTM) mediated quantification of the number of NSMCE2 foci per cell in wt and *Nsmce2*$^{SD/SD}$ MEF in response to MMS (1 mM 1hr; 16 hr recovery) or MMC (0,25 μM 1hr; 16 hr recovery). No significant differences between genotypes could be observed.

Appendix Figure S5. MUS81-dependent SCE in NSMCE2-deficient MEF

SCE events per metaphase on MEF from the indicated genotypes, which were obtained through genetic crosses of *Nsmce2*$^{lox/lox}$ and *Mus81*$^{-/-}$ mice. The *Mus81* knockout strain used for these analyses has been described before (McPherson et al, 2004). Deletion of the conditional *Nsmce2* allele was achieved by infection with a Cre-expressing Adenovirus (AdCre, kind gift of M Barbacid). Data are representative of 2 independent experiments. Error bars indicate s.d.; ***P<0.001.

Appendix Figure S6. Segregation deficiencies observed on NSMCE2-deficient MEF

(A) Quantification of the various segregation deficiencies that can be observed by DAPI staining in *Nsmce2*$^{+/l+}$ and *Nsmce2*$^{lox/lox}$ MEF treated or not with 4-OHT for 8 days. (B) Examples of the types of segregation defects that can be observed on NSMCE2-deficient MEF from (A). Scale bar (white) indicates 2.5 μm.

Appendix Figure S7. Normal DSB-repair kinetics on NSMCE2 deficient MEF

Overall dynamics of DSB repair were assessed through HTM-mediated quantification of the induction and disappearance of 53BP1 nuclear foci in response to IR (5 Gy). No significant differences between the dynamics of 53BP1 foci can be observed between UQ-NSMCE2$^{lox/lox}$ MEF that had been treated (or not) with 4-OHT for 48 hrs previous to the exposure to IR.

Appendix Figure S8. Impact of NSMCE2 deficiency on the developing thymus

Pregnant females were treated at 14.5 dpc for 3 days with intraperitoneal injections of 4-OHT. The image represents the overall loss of cellularity and accumulation of mitotic cells (identified by their reactivity towards an phosphorylated histone H3 Ser 10 antobody) observed on the thymuses of *Nsmce2*$^{lox/lox}$ developing embryos. Some the observed mitotic figures presented evidences of improper chromosome segregation such as anaphase bridges (an example indicated by the black arrow is shown magnified). Scale bar indicates 20 μm.

Appendix Figure S9. 4-OHT-induced deletion of NSMCE2 in adult mice

Western blot analysis of NSMCE2 levels on the indicated organs from *Nsmce2*$^{+/+}$ and *Nsmce2*$^{lox/lox}$ animals carrying the UQ.Cre^{ERT2} transgene, 3 months after being fed with a 4-OHT containing diet. β-ACTIN was used as a loading control.

Appendix Figure S10. Survival of mice deleted for NSMCE2 in adults

Kaplan-Meyer survival curves of *Nsmce2*$^{+/+}$ and *Nsmce2*$^{lox/lox}$ animals carrying the UQ.Cre^{ERT2} transgene after being fed a 4-OHT containing diet that started at weaning. The p value was calculated with the Mantel-Cox long rank test. ***P<0.001.

Appendix Figure S11. Accumulation of micronuclei in NSMCE2 deficient intestines

Representative example of the accumulation of micronuclei that can be observed on the intestinal epithelia from *Nsmce2*$^{+/+}$ and *Nsmce2*$^{lox/lox}$ animals carrying the UQ.Cre^{ERT2} transgene after being fed a 4-OHT containing diet that started at weaning for 3 months. γH2AX was used to facilitate the detection of micronuclei, as reported by (Crasta et al, 2012). Scale bar indicates 100 μm.

Appendix Figure S12. Formation of SMC5/6 complexes on NSMCE deleted B cells

Immunoprecipitation of SMC5 (and IgG, as a control) from a 48 hr culture of B lymphocytes of CD19.Cre transgenic *Nsmce2*$^{+/+}$ and *Nsmce2*$^{lox/lox}$ animals. NSMCE2 and SMC6 levels on the immunoprecipitates were analysed by WB. The image of the ponceau staining is shown as a loading control.

Appendix Figure S13. Absence of co-localization between NSMCE2 and BLM foci

NIH3T3 cells were transfected with a plasmid expressing BLM-YFP (kind gift of I. Hickson). NSMCE2 (red) and BLM (green) foci were induced by treating cells with MMS (1 mM 1hr; 24 hr recovery). DAPI was used to stain DNA. Scale bar indicates 2.5 μm. The images are representative of cells presenting both BLM and NSMCE2 foci.

Appendix Table S1. Percentage of animals or embryos born from *NSMCE2*$^{GT/+}$ *x NSMCE2*$^{GT/+}$ crosses

APPENDIX REFERENCES

Andrews EA, Palecek J, Sergeant J, Taylor E, Lehmann AR, Watts FZ (2005) Nse2, a component of the Smc5-6 complex, is a SUMO ligase required for the response to DNA damage. *Mol Cell Biol* **25:** 185-196

Branzei D, Sollier J, Liberi G, Zhao X, Maeda D, Seki M, Enomoto T, Ohta K, Foiani M (2006) Ubc9- and mms21-mediated sumoylation counteracts recombinogenic events at damaged replication forks. *Cell* **127:** 509-522

Crasta K, Ganem NJ, Dagher R, Lantermann AB, Ivanova EV, Pan Y, Nezi L, Protopopov A, Chowdhury D, Pellman D (2012) DNA breaks and chromosome pulverization from errors in mitosis. *Nature* **482:** 53-58

Kegel A, Betts-Lindroos H, Kanno T, Jeppsson K, Strom L, Katou Y, Itoh T, Shirahige K, Sjogren C (2011) Chromosome length influences replication-induced topological stress. *Nature* **471:** 392-396

McPherson JP, Lemmers B, Chahwan R, Pamidi A, Migon E, Matysiak-Zablocki E, Moynahan ME, Essers J, Hanada K, Poonepalli A, Sanchez-Sweatman O, Khokha R, Kanaar R, Jasin M, Hande MP, Hakem R (2004) Involvement of mammalian Mus81 in genome integrity and tumor suppression. *Science* **304:** 1822-1826

Pebernard S, Schaffer L, Campbell D, Head SR, Boddy MN (2008) Localization of Smc5/6 to centromeres and telomeres requires heterochromatin and SUMO, respectively. *EMBO J* **27:** 3011-3023

Takahashi Y, Dulev S, Liu X, Hiller NJ, Zhao X, Strunnikov A (2008) Cooperation of sumoylated chromosomal proteins in rDNA maintenance. *PLoS Genet* **4:** e1000215

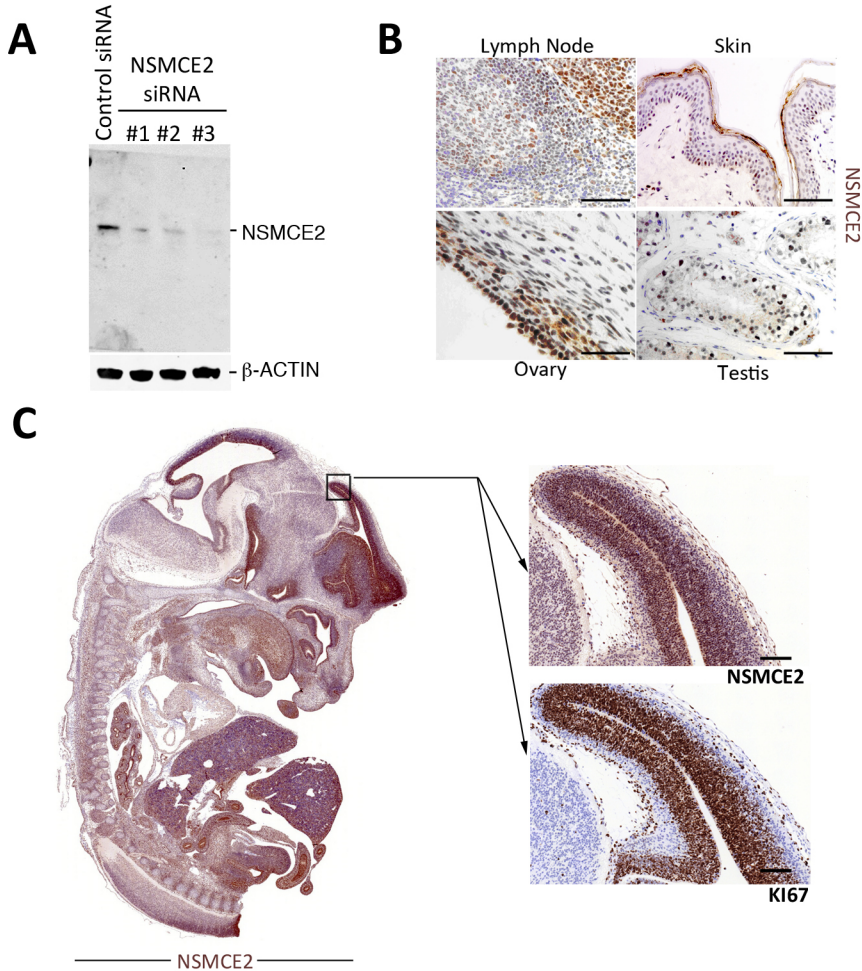
A
Control siRNA
NSMCE2 siRNA
#1 #2 #3
NSMCE2
β-ACTIN
B
Lymph Node
Skin
NSMCE2
Ovary
Testis
C
NSMCE2
NSMCE2
KI67

Jacome *et al* **Fig. S2**

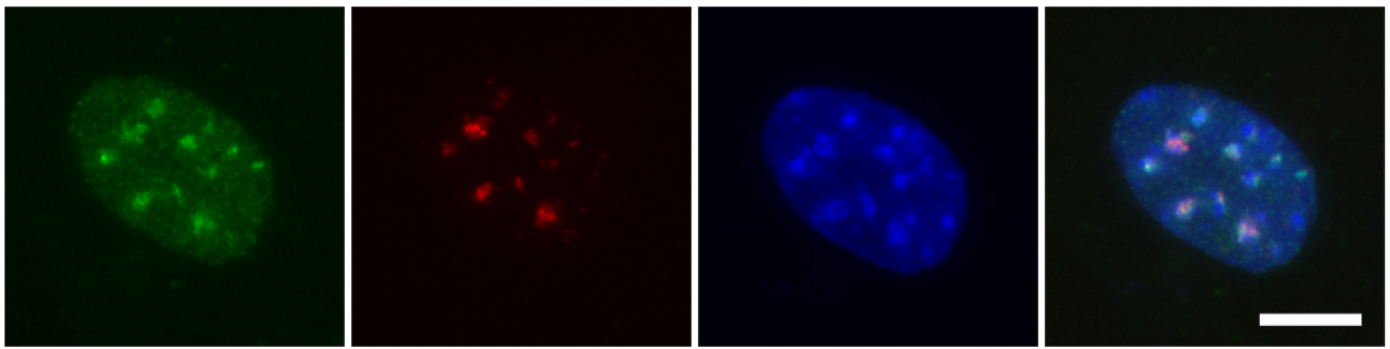

Jacome *et al* **Fig. S3**

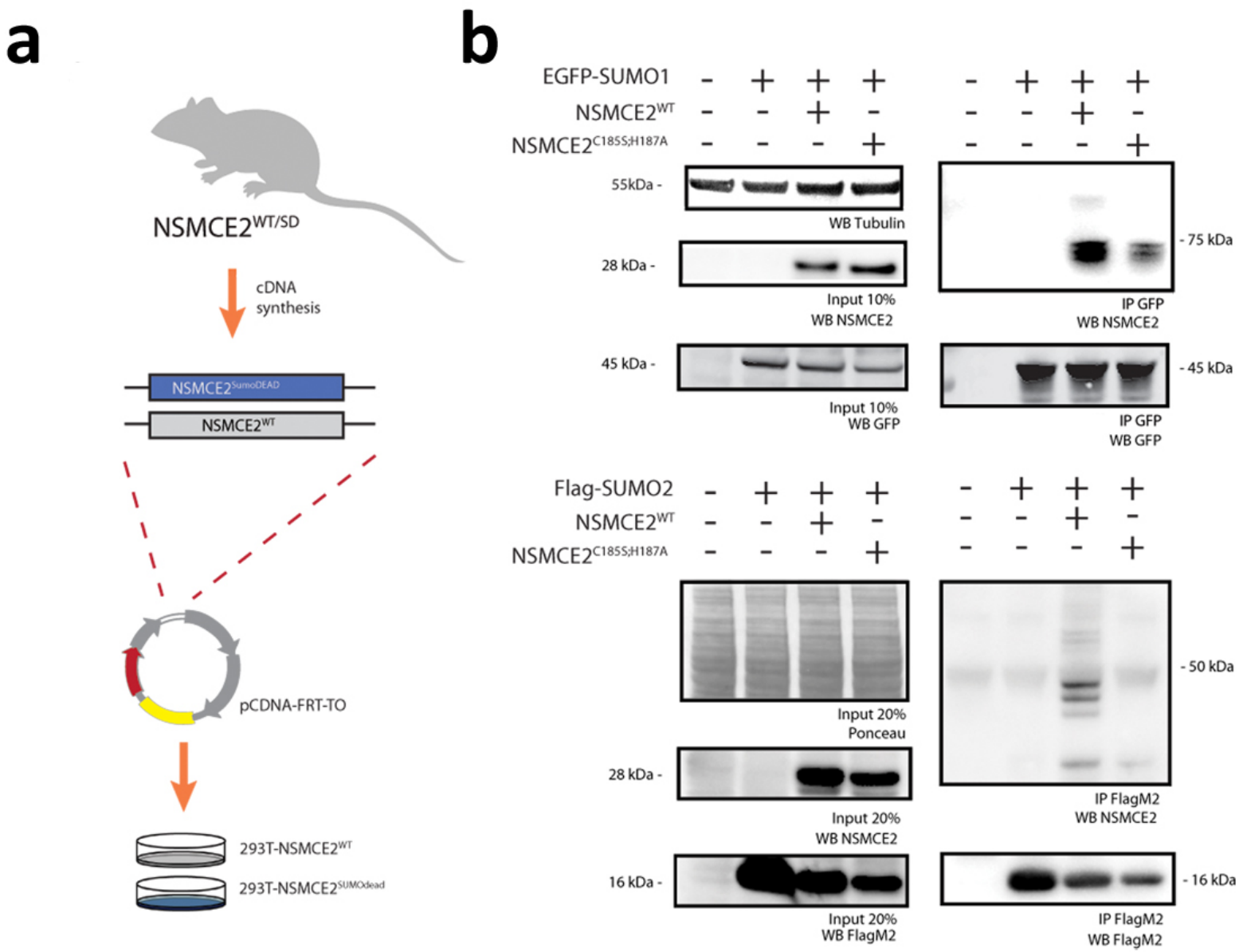

Jacome *et al* **Fig. S4**

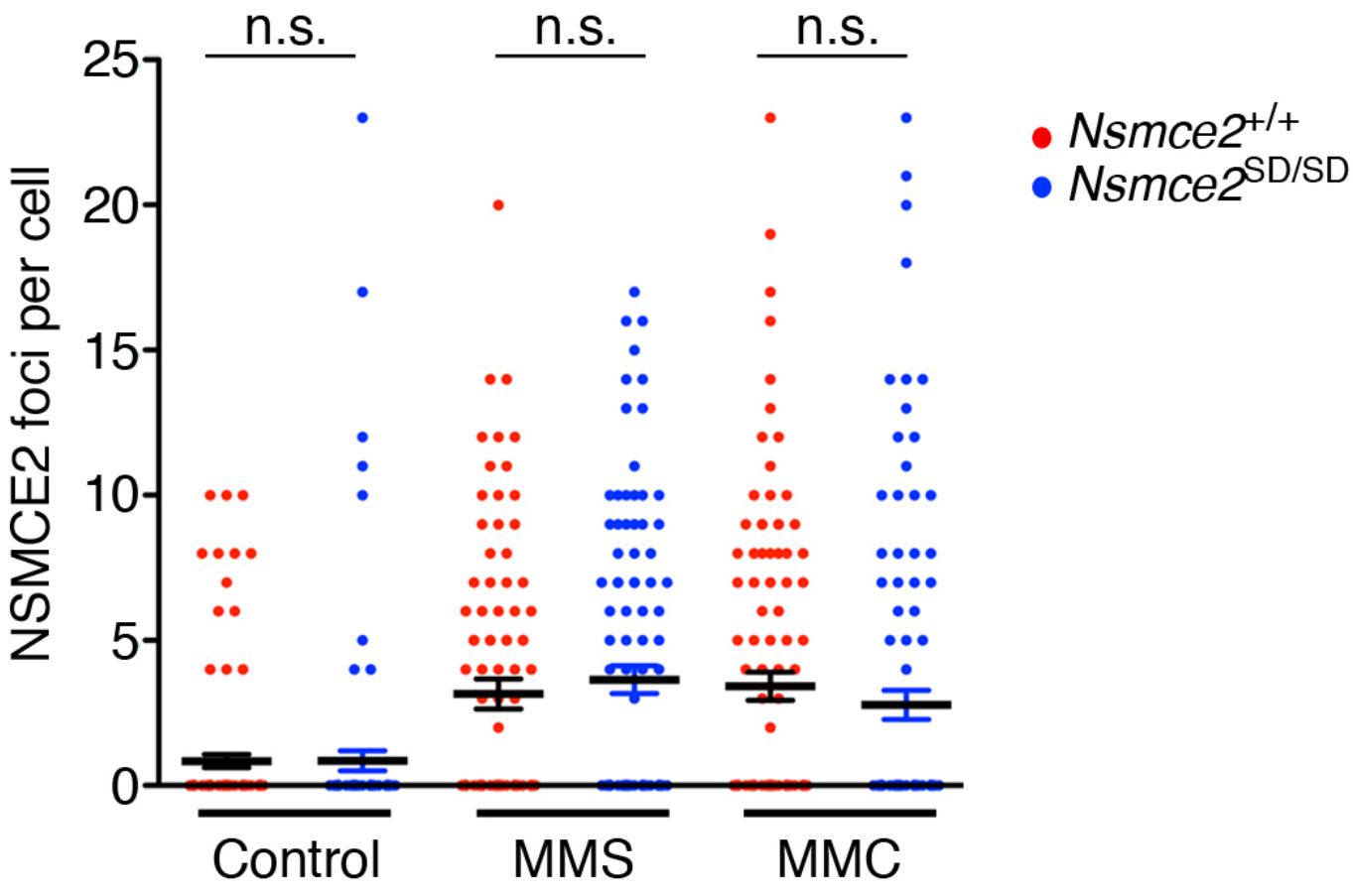

Jacome *et al* **Fig. S5**

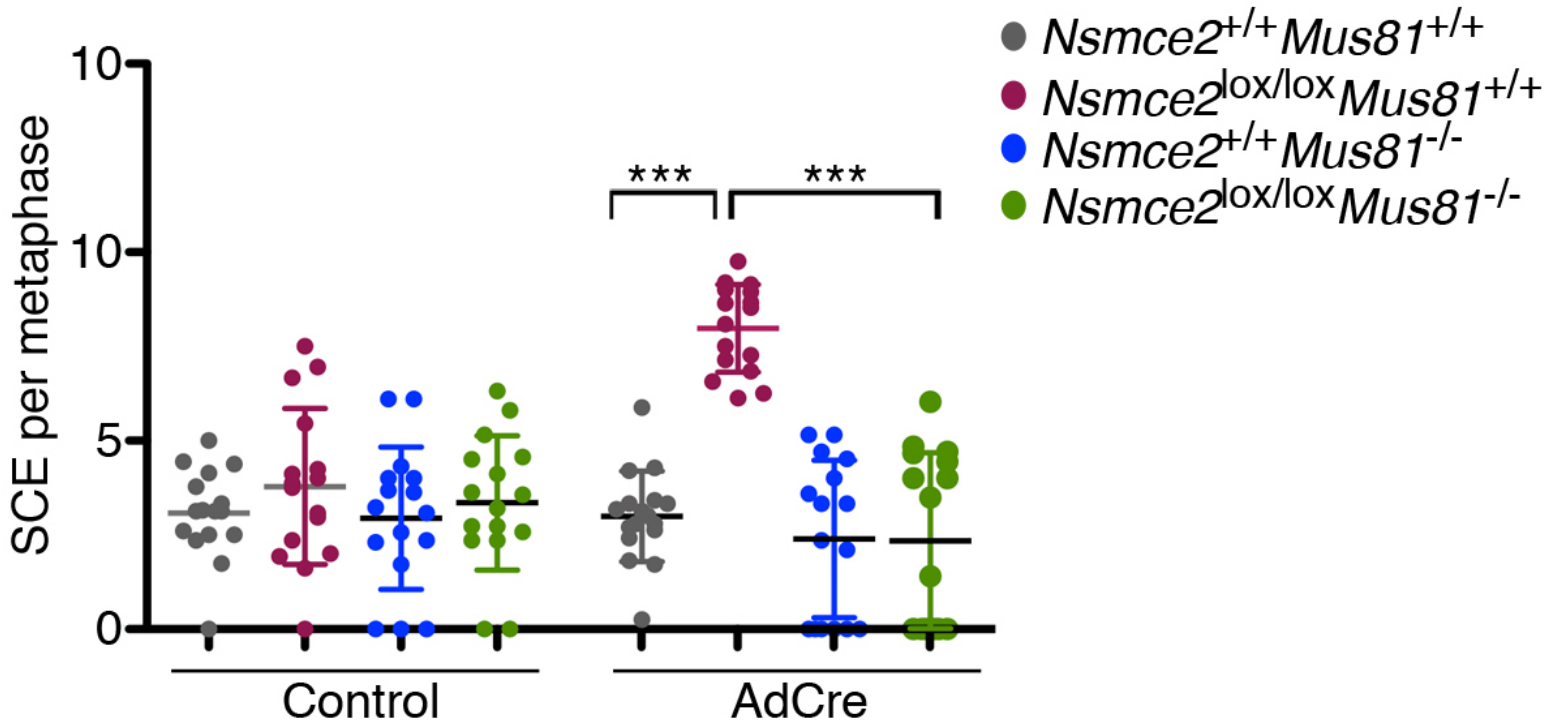

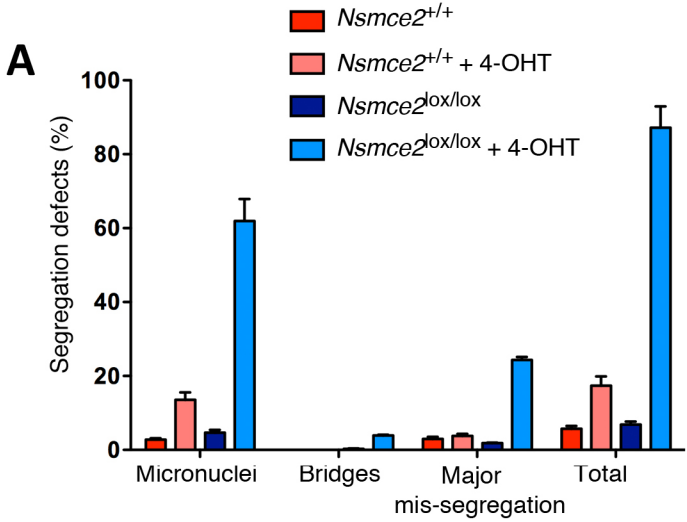
A
Nsmce2+/+
Nsmce2+/+ + 4-OHT
Nsmce2lox/lox
Nsmce2lox/lox + 4-OHT
Segregation defects (%)
100
80
60
40
20
0
Micronuclei
Bridges
Major mis-segregation
Total

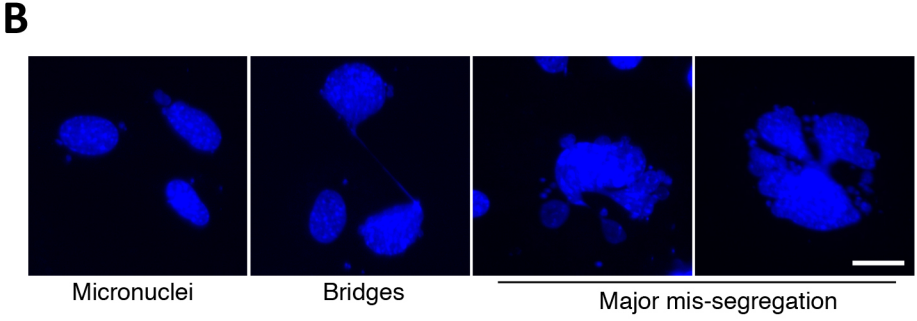
B
Micronuclei
Bridges
Major mis-segregation

Jacome *et al* **Fig. S7**

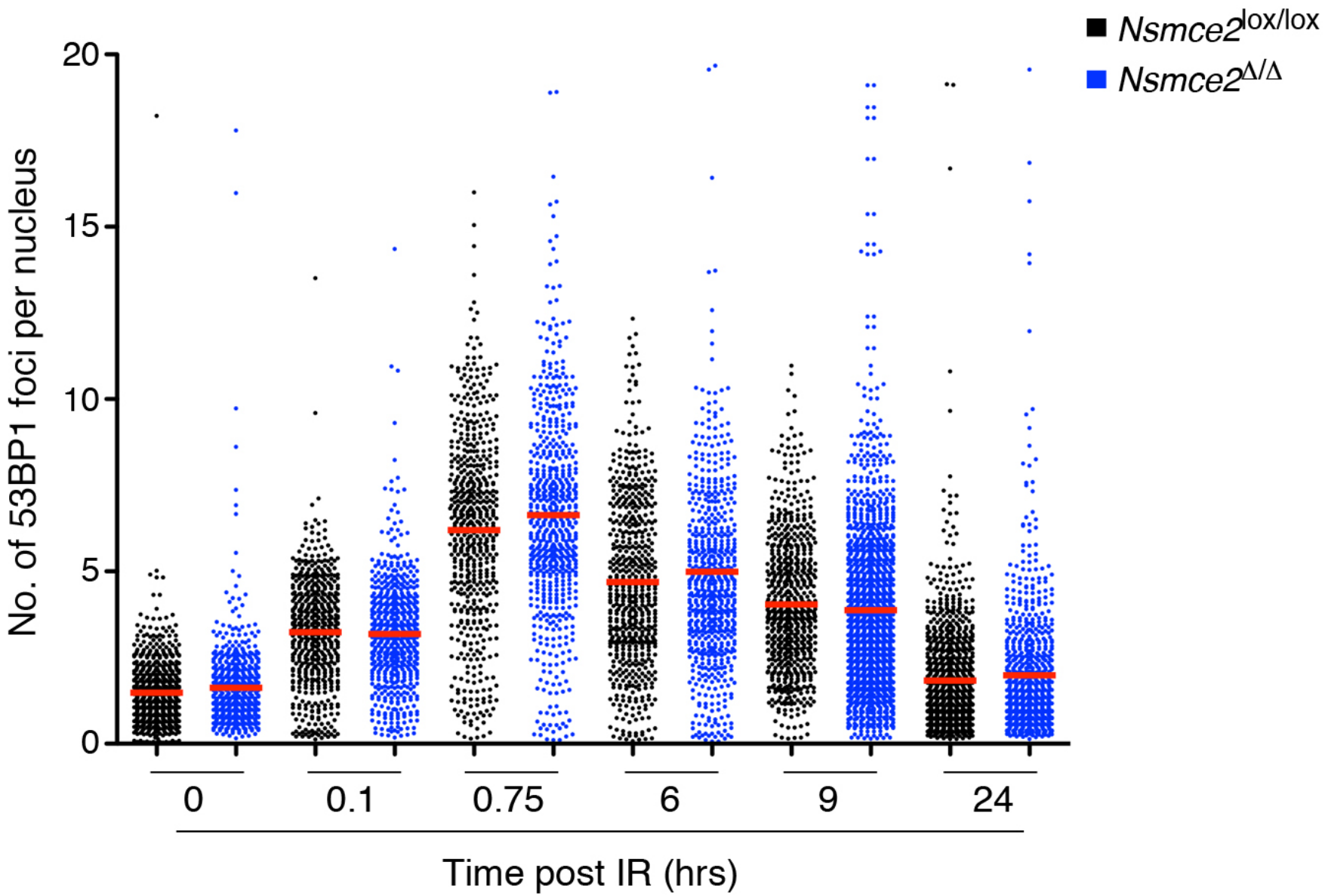

Jacome *et al* **Fig. S8**

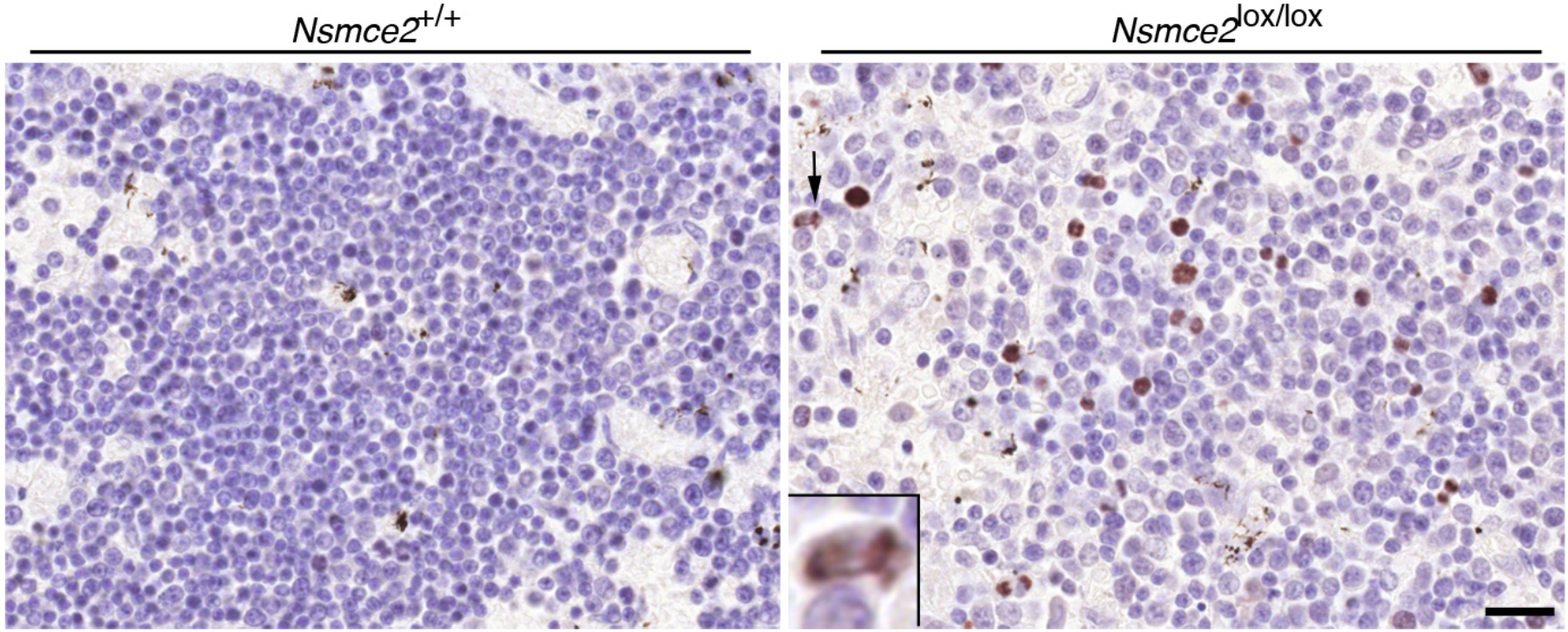

Jacome *et al* **Fig. S9**

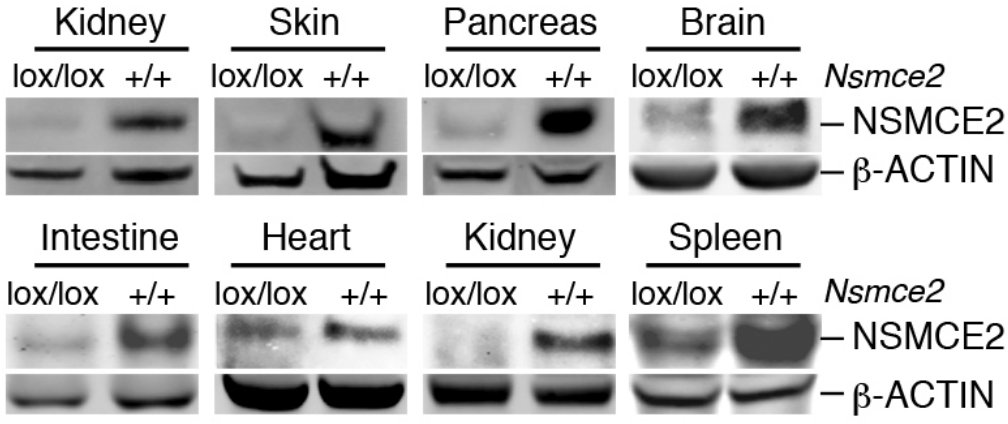

Jacome *et al* **Fig. S10**

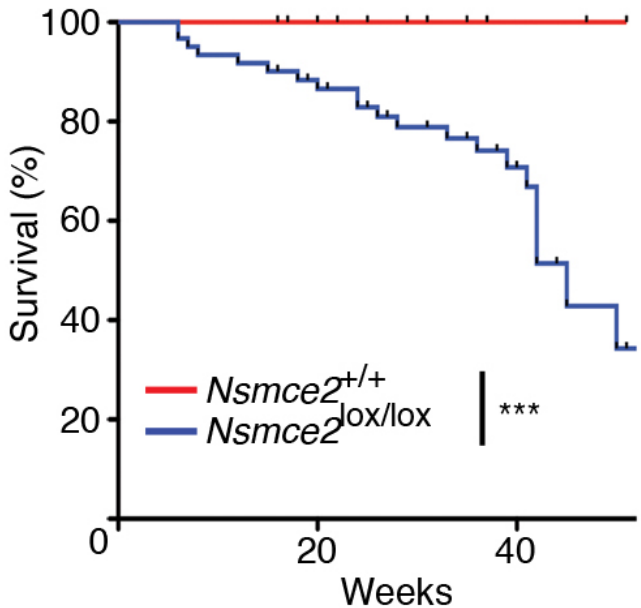

Jacome *et al* **Fig. S11**

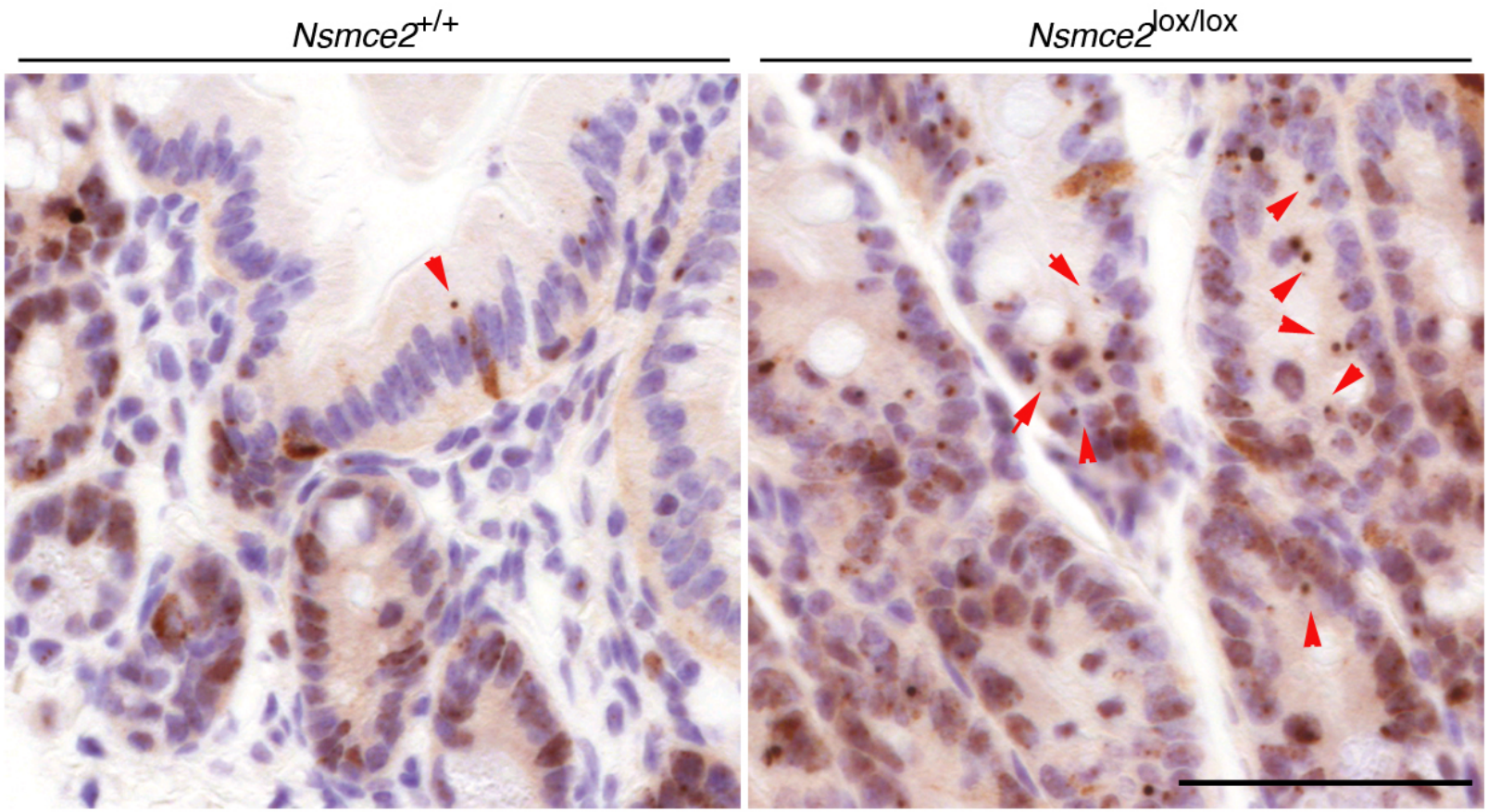

Jacome *et al* **Fig. S12**

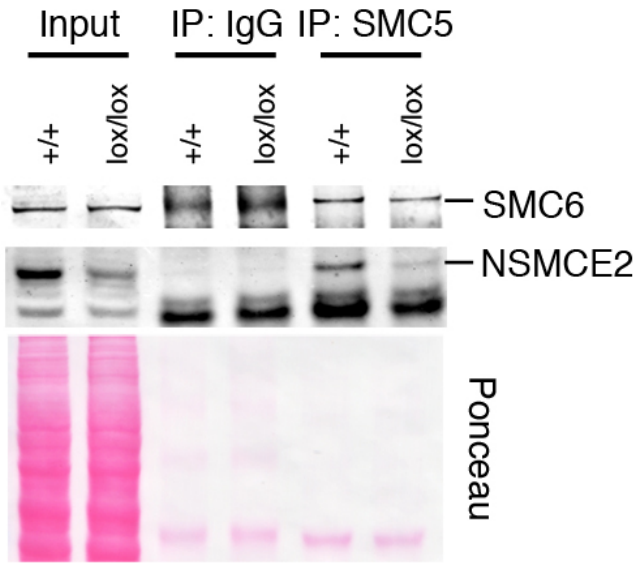

Jacome *et al* **Fig. S13**

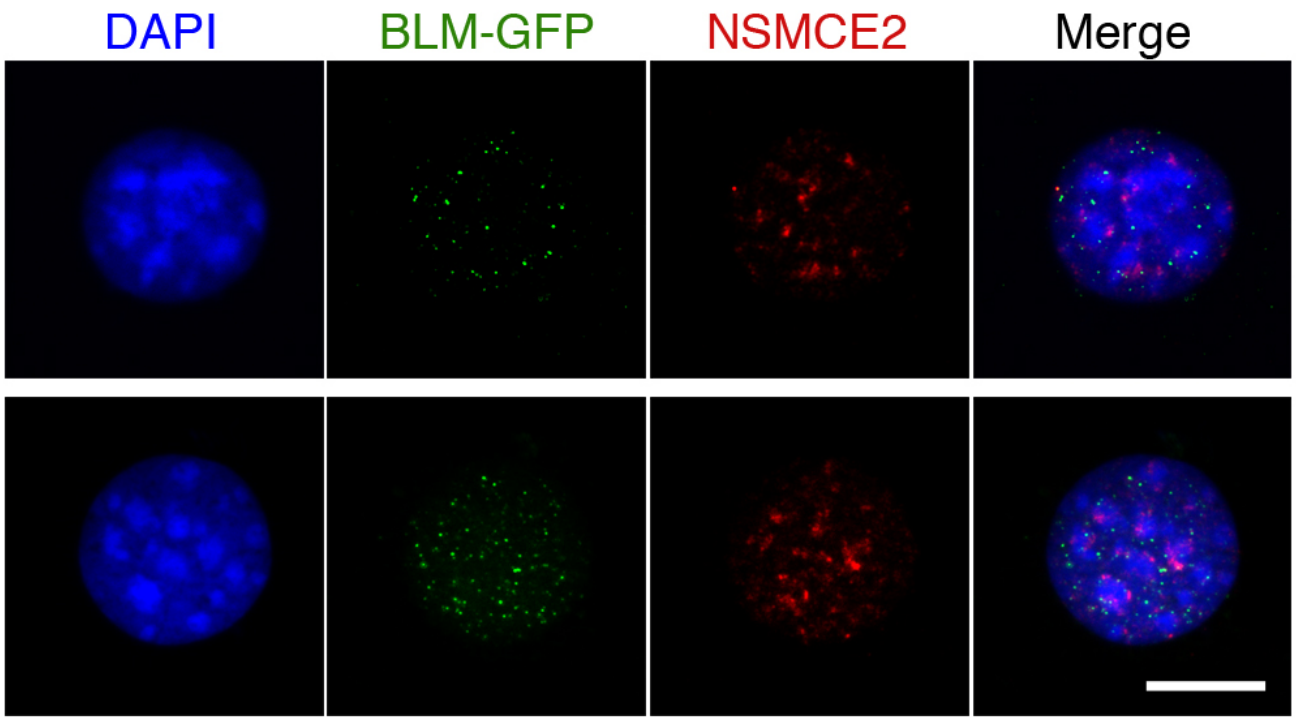

	NSMCE2 +/+	*NSMCE2* GT/+	NSMCE2 GT/GT	*(n)*
Adult	38,2	61,8	0	*123*
e13.5	40	60	0	*20*
e10.5	23,5	76,5	0	*17*
e2.5	28,9	48,9	22,2	*45*

Table S1. Percentage of animals or embryos born from *NSMCE2*$^{GT/+}$ x *NSMCE2*$^{GT/+}$ crosses